Elsevier Editorial System(tm) for Food Research International
Manuscript Draft

Manuscript Number:

Title: DEVELOPMENT AND CHARACTERIZATION OF FOOD-GRADE ELECTROSPUN FIBERS FROM AMARANTH PROTEIN AND PULLULAN BLENDS

Article Type: Research Article

Keywords: Electrospinning; amaranth protein; pullulan; encapsulation; ultrathin fibers

Corresponding Author: Dr. Amparo Lopez-Rubio,

Corresponding Author's Institution:

First Author: Marysol Aceituno-Medina

Order of Authors: Marysol Aceituno-Medina; Sandra Mendoza; Jose M Lagaron; Amparo Lopez-Rubio

Abstract: In this work, novel ultrathin electrospun fibers from different blends of amaranth protein isolate (API) and the carbohydrate polymer pullulan, with or without the surfactant Tween80, have been developed and characterized. The solution properties and molecular organization of the electrospun structures were studied and correlated with the morphology of the obtained fibers. The presence of pullulan in the blends resulted in increased viscosity and lower conductivity of the solutions, related to a better chain entanglement and decrease in the polyelectrolyte protein character, respectively, both factors needed for fiber formation. Infrared spectral changes indicated that defect-free fibers were correlated with extended α-helical protein structures, which for the blends with greater protein contents, was only obtained upon surfactant addition. The thermal stability of the hybrid fibers was better than that of pure API and slightly increased upon surfactant addition, while the water stability of the blends was highly dependent on fiber composition. These structures have a great potential for the encapsulation of bioactives for functional food applications.

HIGHLIGHTS

- Novel ultrathin electrospun fibres of amaranth protein and pullulan were developed
- Surfactant was needed to obtain defect-free fibres for high protein content blends
- FTIR can be unequivocally used to distinguish between defect-free and beaded fibres
- Thermal stability of the blends slightly improved with respect that of pure protein
- Water sensitivity of the fibres was highly dependent on blend composition

# DEVELOPMENT AND CHARACTERIZATION OF FOOD-GRADE ELECTROSPUN FIBERS FROM AMARANTH PROTEIN AND PULLULAN BLENDS

Marysol Aceituno-Medina[1], Sandra Mendoza [1], José María Lagaron[2], Amparo López-Rubio[2*]

[1] Dept. de Investigación y Posgrado en Alimentos, Facultad de Química, Universidad Autónoma de Querétaro, 76010, Querétaro, México

[2] Novel Materials and Nanotechnology Group, IATA-CSIC, Avda. Agustin Escardino 7, 46980 Paterna (Valencia), Spain

*Corresponding author: Tel.: +34 963900022; fax: +34 963636301

E-mail address: amparo.lopez@iata.csic.es (A. López-Rubio)

**Abstract**

In this work, novel ultrathin electrospun fibers from different blends of amaranth protein isolate (API) and the carbohydrate polymer pullulan, with or without the surfactant Tween80, have been developed and characterized. The solution properties and molecular organization of the electrospun structures were studied and correlated with the morphology of the obtained fibers. The presence of pullulan in the blends resulted in increased viscosity and lower conductivity of the solutions, related to a better chain entanglement and decrease in the polyelectrolyte protein character, respectively, both factors needed for fiber formation. Infrared spectral changes indicated that defect-free fibers were correlated with extended α-helical protein structures, which for the blends with greater protein contents, was only obtained upon surfactant addition. The thermal stability of the hybrid fibers was better than that of pure API and slightly increased upon surfactant addition, while the water stability of the blends was highly dependent on fiber composition. These structures have a great potential for the encapsulation of bioactives for functional food applications.

**Keywords**

Electrospinning, amaranth protein, pullulan, encapsulation, ultrathin fibers

**Abbreviations**

API: Amaranth protein isolate

## 1. Introduction

In today's world, nutraceutical food is considered not only a source of nutrients but also as having to contribute to the health of consumers. However, the effectiveness of nutraceutical products in preventing diseases depends on preserving the bioavailability of the active ingredients (Bell, 2001). In this regard, the range of applications for micro- and nanoencapsulation in the food industry has been increasing because of the many advantages that these technologies can confer to the encapsulated material. These include enhancing the stability under conditions encountered in food processing (temperature, oxygen, light) or in the gastrointestinal tract (pH, enzymes). Even though there are various types of encapsulation technologies, the production of nanofibers through the electrospinning technique has received much attention lately. Electrospinning is a process that produces continuous polymer fibers with diameters in the submicrometer range through the action of an external electric field imposed on a polymer solution or melt (Reneker & Chun, 1996). Applications of electrospun nanofibers for food and agricultural systems are relatively scarce. This is probably because fibers are made primarily from synthetic polymers. However, the progress in the production of nanofibers from food biopolymers has increased considerably. With respect to encapsulation for food applications, this technique has only very recently been applied to encapsulate antioxidants (Li, Lim, & Kakuda, 2009; Lopez-Rubio & Lagaron, 2012; Torres-Giner, Martinez-Abad, Ocio, & Lagaron, 2010) and probiotic bacteria (Heunis, Botes, & Dicks, 2010; Lopez-Rubio, Sanchez, Sanz, & Lagaron, 2009; Lopez-Rubio, Sanchez, Wilkanowicz, Sanz, & Lagaron, 2012). This is mainly due to the challenges encountered for electrospinning certain biopolymers, like for instance some proteins (i.e. egg albumen, soy protein) because of their complex macromolecular and

three-dimensional structures in conjunction with strong inter- and intramolecular forces. Some strategies to improve the spinnability of these biopolymers rely on the use of surfactants (Kriegel, Kit, McClements, & Weiss, 2009), plasticizers (Nie et al., 2008) or reducing agents (Aceituno-Medina, Lopez-Rubio, Mendoza, & Lagaron, 2013). The difficulties in generating electrospun fibers from certain biopolymers have also been overcome through blending with readily spinnable polymers in solution (Wongsasulak, Patapeejumruswong, Weiss, Supaphol, & Yoovidhya, 2010). In a previous work, the ability of an amaranth protein isolate (API) to generate electrospun micro- and submicron structures was demonstrated (Aceituno-Medina et al., 2013). Amaranth (*Amaranthus hypochondriacus*) is considered a highly nutritious food in México and other Central American countries. The grain has high protein content (17%), and its amino acid composition is close to the optimum amino acid balance required in the human diet (Schnetzler & Breen, 1994; Teutónico & Knorr, 1985), moreover it is a low cost material, compared with other proteins. Contrarily to most common grains, the proteins in amaranth contain very little or no storage prolamin proteins, which are the main storage proteins in cereals, and also the toxic proteins in celiac disease (Drzewiecki *et al.,* 2003; Gorinstein *et al.*, 2002). However, amaranth proteins alone dissolved in food contact permitted solvents could not form electrospun fibers (Aceituno-Medina et al., 2013) and, thus, the aim of the present work was to focus on the production of electrospun fibers through blending the amaranth protein isolate material with a spinnable carbohydrate polymer. Pullulan was the carbohydrate selected, not only because it has been previously shown to produce ultrathin electrospun fibers (Karim et al., 2009), but also because it is an edible polymer (Kimoto, Shibuya, & Shiobara, 1997), capable of forming hydrogen bonds with proteins (Gounga, Xu, & Wang, 2007), it is resistant to mammalian amylases (which could be an advantage

for encapsulation applications), provides few calories and it is considered as dietary fiber in rats and humans (Yoneyama et al., 1990). For all these reasons, the objective of this study was to evaluate the feasibility of producing electrospun fibers from different API-pullulan blends and to evaluate the influence of Tween 80 (non-ionic surfactant) on the morphology and molecular organization of the electro-deposited material. These ultrathin fibers could be potentially used for nutraceutical delivery in food applications.

## 2. Materials and methods

### 2.1 Materials

Formic acid of 95% purity, non-ionic surfactant, polyoxyethylene sorbitan monooleate (Tween 80) and pullulan ($M_w$~100000) were supplied by Sigma-Aldrich. The commercial amaranth protein concentrate (*Amaranthus hypochondriacus* L. Revancha variety) was supplied by Nutrisol (Hidalgo, Mexico). The Amaranth Protein Isolate (API) was prepared based on the methodology previously reported by Martínez and Añón (1996) with some modifications. The protein isolate prepared under these conditions consisted in a mixture of different proteins with molecular weights ranging from 10-83 kDa (Aceituno-Medina et al., 2013). Briefly, the commercial amaranth protein concentrate (APC) was defatted with hexane for 12 h (10% w/v suspension). Then, the amaranth protein concentrate was suspended in water and its pH was adjusted to 9 with a 2 N NaOH solution. The suspension was stirred for 30 min at room temperature and, then, centrifuged 20 min at 9000 *g*. Then, the supernatant was adjusted to pH 5 with 2 N HCl and centrifuged at 9000 g for 20 min at 4°C. The pellet was resuspended in water, neutralized with 0.1 N NaOH and freeze-dried. The protein content was determined by the Kjeldahl technique (AOAC, 1996) using a conversion factor of 5.85.

### 2.2 Preparation of polymer solutions for electrospinning

API and pullulan blends were dissolved in 95% formic acid. The polymer content in solution was kept constant at 20% w/v. The polymers were blended at different proportions (50:50, 60:40, 70:30 and 80:20 w/w) of API and pullulan, respectively. The solutions were

prepared with and without addition of Tween 80 (~20 wt. % with respect to the API content). Each solution was gently stirred to ensure a complete dissolution.

### 2.3 Characterization of the polymer solutions

The viscosity of the polymer solutions was determined using a rotational viscosity meter Visco Basic Plus L from Fungilab S.A. (San Feliu de Llobregat, Spain) using a Low Viscosity Adapter (LCP). The surface tension of the polymer solutions was measured using the Wilhemy plate method in a EasyDyne K20 tensiometer (Krüss GmbH, Hamburg, Germany). The conductivity of the solutions was measured using a conductivity meter XS Con6 (Labbox, Barcelona, Spain). All measurements were made in triplicate at 25ºC.

### 2.4 Electrospinning of the blends

The electrospinning apparatus, a FluidNatek® instrument, trademark of BioInicia S.L. (Valencia, Spain), equipped with a variable high voltage 0–30 kV power supply was used. The anode was attached to a stainless-steel needle with internal diameter 0.9 mm that was connected through a PTFE wire to the biopolymer solutions kept in a 5 ml plastic syringe. The syringe was disposed horizontally lying on a digitally controlled syringe pump while the needle was vertically directed towards the collector. The needle was connected to the emitting electrode of positive polarity of the high voltage power supply. The electrospun structures were collected on an aluminum foil sheet attached to a copper grid used as collector. All of the electrospinning experiments were carried out at room temperature in air. The electrospinning environmental conditions were maintained stable at 24°C and 60% RH by having the equipment enclosed in a specific chamber with temperature and humidity control. The target was placed 10 cm from the capillary tip. The syringe pump delivered

polymer solution at a controlled feed rate of 0.4 ml/h, while the voltage was maintained at 22 and 15 kV, for polymer solutions with and without surfactant, respectively.

**2.5 Scanning Electron Microscopy (SEM)**

The morphology of the electrospun fibers was examined using SEM (Hitachi S-4100) after sputtering the samples with a gold–palladium mixture under vacuum. All SEM experiments were carried out at an accelerating voltage of 15 kV. Fiber diameters of the electrospun fibers were measured by means of the Adobe Photoshop 7.0 software from the SEM micrographs in their original magnification.

**2.6 Attenuated total reflectance infrared spectroscopy (ATR-FTIR)**

ATR-FTIR spectra were collected in a controlled chamber at 24°C and 40% RH coupling the ATR accessory GoldenGate of Specac Ltd. (Orpington, UK) to a Bruker (Rheinstetten, Germany) FTIR Tensor 37 equipment. All the spectra were collected by averaging 20 scans at 4 $cm^{-1}$ resolution. Analysis of the spectral data was performed using Grams/AI 7.02 (Galactic Industries, Salem, NH, USA) software.

**2.7 Thermogravimetric Analysis (TGA)**

Thermogravimetric analysis (TG) curves were recorded with a TA Instruments model Q500 TGA. The samples (ca. 10 mg) were heated from 50 to 800°C with a heating rate of 5°C/min under nitrogen atmosphere. Derivative TG curves (DTG) express the weight loss as a function of temperature.

## 2.8 Effect of Relative Humidity (RH) and water resistance of the electrospun fibers

To study the relative humidity effects on the stability and morphology of the fibers, immediately after spinning, the fiber mats API:pullulan 50:50 and 80:20 with Tween80 were stored at 25°C in a glass desiccator at 100% RH. Samples were retrieved from the desiccators after 30 minutes and analyzed using SEM. Moreover, in order to estimate pullulan potential losses as a consequence of its hydrophilic character, samples of ~1mg fibers corresponding to the 50:50 and 80:20 blends with Tween80 were immersed in distilled water for 5, 20, 30 and 60 minutes. Afterwards, they were dried under vacuum at 60ºC, weighed and analyzed using FTIR spectroscopy.

## 2.10 Statistical analysis

One-way analysis of the variance (ANOVA) was performed using XLSTAT-Pro (Win) 7.5.3 (Addinsoft, NY) software package. Comparisons between samples were evaluated using the Tukey test ($\alpha = 0.05$).

## 3. Results and discussions

### 3.1 Optimization of the electrospinning conditions for the API:pullulan blends

Pullulan is a carbohydrate polymer able to produce electrospun fibers from aqueous solutions and, thus, initially we investigated the spinnability of binary mixtures of pullulan solutions dissolved in water and API solutions in formic acid with concentrations of 20% (w/w) and 10% (w/w), respectively. Even though different mass compositions of API to pullulan solutions were examined, a clear phase separation was detected after only 15-25 minutes of agitation. One of the main challenges of electrospinning biopolymers is to obtain solutions which are relatively stable with time, in order to have a continuous process for electrospun fiber production (this is especially important when scaling up the process). Therefore, the previous blends were discarded. As an alternative, the spinnability of pullulan in formic acid was studied. The carbohydrate was also soluble in this solvent and two different concentrations were examined, i.e. 10% and 20% w/v. While pullulan solutions at 10% (w/v) gave rise to beaded fibers, which could be attributed to the lack of sufficient polymer chain entanglement at this concentration (Buchko, Chen, Shen, & Martin, 1999; Wongsasulak et al., 2010), continuous fibers were obtained from the solutions containing 20% of pullulan (see Figure A.1 in the Appendices).

As a consequence, for blend preparation, both the amaranth protein (API) and the carbohydrate polymer (pullulan) were dissolved in formic acid. Polymer blend solutions with API:pullulan contents of 50:50, 60:40, 70:30 and 80:20 (w/w) were prepared and left to stand at ambient conditions for 72 h in order to detect any potential phase separation. Results indicated that, in all cases, the solutions were properly mixed and stable with time, which could be attributed to the formation of protein-polysaccharide soluble complexes through the formation of hydrogen bonds (C=O----HO, OH----OH, HO----HN),

hydrophobic interactions and/or ionic bonds (Gounga et al., 2007; McClements, 2006; Tolstoguzov, 1991). An indirect way to demonstrate the compatibility between API and pullulan was through comparison of the morphologies obtained using only pullulan with a concentration of 10% (w/v) in formic acid and blends of API-pullulan at different ratios. While as previously shown, beaded electrospun fibers were generated from pullulan solutions at 10% (w/v) (cf. Fig. A.1a in the Appendices), uniform fibers were obtained from the blend API:pullulan 70:30, which only contained 8% w/v of pullulan. Therefore, it appears that the addition of API in the blend solutions improved the entanglement through the interactions between both biopolymers (cf. Figure 1).

INSERT FIGURE 1 ABOUT HERE

Figure 1 shows the scanning electron microscopy images of the various API:pullulan blends. Continuous fibers with diameters of around 300 nm were obtained from mixtures 50:50 and 60:40 (Fig. 1A and C). The blend containing 70% of API gave rise to uniform electrospun fibers with similar size and few bead defects (Fig. 1E), while greater amounts of API in the blends (i.e. 80%), resulted in less stable electrospinning, generating electrospun fibers with numerous bead defects (cf. Fig. 1G).

### 3.2 Effect of surfactant addition on the morphology of electrospun API:pullulan structures

In order to improve the spinnability of the blends and to obtain more homogeneous fiber structures improving the degree of entanglement between the protein and carbohydrate polymers, a food-grade non-ionic surfactant (Tween 80) was added at 20% (w/w), as this

percentage was previously seen to greatly improve the electrospinning process of amaranth protein isolate solutions (Aceituno et al., 2013).

Addition of Tween 80 significantly improved the fiber morphology for the blends with greater protein content, resulting in defect-free smooth electrospun fibers for the 70:30 and 80:20 API:pullulan compositions (cf. Fig. 1F and 1H, respectively) and more homogeneous fiber diameters were obtained for all the studied compositions (cf. Table 1). The use of surfactants for improving electrospun fiber morphology has been previously reported (Peng et al., 2008; Jung, Kim, Lee, & Park, 2005). Addition of Tween 80 may facilitate the dispersion of API molecules throughout the solutions, consequently leading to changes in the flow behavior of the mixed solutions and, thus, improving the productivity of the electrospinning process (Kriegel et al., 2009).

Both the more homogeneous fiber diameters obtained and the development of defect-free electrospun fibers when incorporating the surfactant could be explained by the binding of surfactant monomers to the protein backbone either through hydrophobic interactions or hydrogen bonding, forming a complex which retained its overall charge but affecting intramolecular interactions and conformation of the protein. As previously hypothesized, interaction between surfactant and protein may result in a more open molecular structure which may help to establish interactions with the carbohydrate polymer pullulan, thus, decreasing the critical entanglement concentration and, thereby, facilitating electrospinning (Kriegel et al., 2009).

### 3.3 Correlation between physical properties of blend solutions and morphology of electrospun fibers

As it has been noted by several authors, the physicochemical properties of polymer solutions such as viscosity, surface tension and conductivity play a key role in the formation of continuous fibers (Kriegel et al., 2009; Wongsasulak, Kit, McClements, Yoovidhya, & Weiss, 2007). The solution properties together with the mean fiber diameter for the various protein/carbohydrate compositions are compiled in Table 1.

INSERT TABLE 1 ABOUT HERE

In general, it can be observed that increasing the amount of the carbohydrate polymer in the blend solutions led to an increase in the apparent viscosity (thus confirming that pullulan addition enhanced chain entanglement needed for fiber formation) and decreased the conductivity, suggesting that there might be interactions between both biopolymers leading to a decrease in the polyelectrolyte character of the protein. Surface tension remained almost constant for the different protein/carbohydrate ratios. Regarding fiber diameter, no significant changes were observed across the compositions, except for the blend with greater protein content, which contained many bigger bead defects along the fibers. Although, the development of continuous fibers using ratios of 50:50 and 60:40 can be partially associated to the effect of pullulan addition on solution properties (specifically viscosity and conductivity) the main contribution of pullulan to the electrospinning process is to act as a plasticizer facilitating orientation and flow of API by uncoiling and wrapping around API chains (Kriegel et al., 2009). Consequently, as the polyelectrolyte properties of the protein decreased upon interaction with the carbohydrate, the number of entanglements increased, facilitating the formation of defect-free fibers. However, the plasticizing effect of

pullulan was insufficient for formation of homogeneous fibers for the formulation containing the greatest protein content (i.e. 80:20).

Although not statistically significant, a general trend of increased average fiber diameter was observed upon addition of Tween80, which might be related to the slight increase in apparent viscosity and lower conductivity observed for the solutions containing the surfactant (cf. Table 1). This increase in the apparent viscosity of the solutions again seems to highlight the enhancement of chain entanglements or improved interactions between the protein and the carbohydrate biopolymers.

### 3.4 Changes in molecular order of the electrospun ultrathin fibers from API:pullulan blend solutions by ATR-FTIR.

Figure 2 shows the infrared spectra of electrospun structures obtained from mixtures of API:pullulan. For clarity purposes, only the spectra from the blends API:pullulan 50:50 and 80:20 with and without surfactant have been included in this figure. The spectra of the electrospun structures from the pure components (i.e. API and pullulan) are also included for comparison purposes. The spectra of the blends obtained through electrospinning clearly indicated that the ultrathin fibers were composed of both API and pullulan. Moreover, a more detailed analysis of band position and shape revealed that there was some chemical interaction between both biopolymers, as many characteristic bands from both the protein and the carbohydrate polymer were significantly displaced as further commented below.

INSERT FIGURE 2 ABOUT HERE

In the FTIR range of the OH and NH stretching vibrations (i.e. from ~3000 to ~3700 $cm^{-1}$) it was observed that the maximum of this band in the blends was between the maximum of the band for pullulan (~3360 $cm^{-1}$) and the maximum for the amaranth protein structures (~3280 $cm^{-1}$, cf. dashed line in Figure 2), but closer to the maximum of the NH stretching band from API. Moreover, in all the blends a broadening of the band was observed with a marked increase in intensity in the range 3340-3600 $cm^{-1}$, which could be ascribed to a greater number of intermolecular hydrogen bonds probably due to the interactions between the OH groups from pullulan and the NH groups from API.

In the spectra from the blends, characteristic peaks for the amaranth protein isolate (API) were identified at ~1637 $cm^{-1}$ and ~1525 $cm^{-1}$, which correspond to the amide I and II regions, respectively. The amide I region arises from the peptide backbone C=O stretching mode and has been widely used to study protein folding, unfolding and aggregation with infrared spectroscopy due to its sensitivity to secondary structure of proteins (Barth, 2007), while the amide II region mainly corresponds to stretching vibrations of C-N and bending of N-H bonds and it is conformationally sensitive. On the other hand, vibrational bands in the region from 800 to 1200 $cm^{-1}$ are characteristic from carbohydrates. Absorption bands at 775, 850 and 932 $cm^{-1}$ are characteristic of α-(1,4) glycosidic bonds, α-glucopyranoside units and α-(1,6) glycosidic bonds, respectively (Prasad, Guru, Shivakumar, & Sheshappa Rai, 2012). The region between 950 and 1250 $cm^{-1}$ corresponds to highly coupled modes mainly arising from C-C, C-O, C-H stretching and COH bending modes (Lopez-Rubio, Flanagan, Shrestha, Gidley, & Gilbert, 2008). In order to qualitatively estimate the fiber compositions, the ratio between the bands corresponding to the amide II from API (at ~1539 $cm^{-1}$) and the band from the α-glucopyranoside units from pullulan (at ~850 $cm^{-1}$)

was calculated and the results can be seen in Figure A.2 in the Appendices, which showed that both the protein and the carbohydrate were effectively incorporated into the electrospun fibers, following the ratio of these two bands a linear relationship with the protein content of the blends.

As mentioned before, amide I and II bands from the protein can also provide very useful information about the conformation of the polymeric chains which, at the same time, would help explaining the morphology of the electrospun structures. Figure 3 shows the FTIR spectra in the range of the amide I and II bands.

INSERT FIGURE 3 ABOUT HERE

From this Figure, it can be clearly seen that for most of the blends, the maximum of amide I band for pure API, placed around 1639 $cm^{-1}$and which corresponds to the absorption of intramolecular β-sheet structures, was displaced towards higher wavenumbers being centered around 1650 $cm^{-1}$, assigned to α-helical structures. Only the blends with greater API content were not displaced at all (this was the case for the API:pullulan 80:20 blend), or the absorption band was broader (in the case of the API:pullulan 70:30 blend) indicating, in this latter case, the coexistence of α-helical and β-sheet structures. These spectral features coincide with the fact that these two compositions were mostly capsular morphologies or beaded fibers, respectively. When the surfactant Tween80 was added to these blends, the amide I bands from the structures obtained thereof were centered around 1650 $cm^{-1}$, confirming the hypothesis that the surfactant contributed to uncoil the protein chains, attaining an extended conformation and, thus, giving rise to defect-free fibers.

Regarding the amide II band, it also presented a shift in position and band shape for the blends in comparison with the structures obtained from pure API. While in the latter case a broad band with two maximums at ~1519 and 1529 $cm^{-1}$ were observed, in the blends API:pullulan 50:50 and 60:40 a narrower band centered around 1540 $cm^{-1}$ was apparent. The other two blends with greater protein content, showed wider bands with the maximum located between the pure API structures and the low protein content blends. In a similar way as the observations made for the amide I band, upon surfactant addition, the amide II band position shifted towards 1540 $cm^{-1}$ and got narrower. This shift of the amide II band towards higher wavenumbers might be indicating, as observed by other authors (Wu, Zhong, Li, Shoemaker, & Xia., 2013), that a strong interaction between the amino groups from the protein and the hydroxyl groups from the carbohydrate took place, fact that could also had favored electrospun fiber formation.

**3.5 Thermal stability of electrospun nanofibers.**

The thermal stability of electrospun API/pullulan ultrathin fibers was evaluated through TGA. Figure 4 shows the DTG curves of pure API, pullulan, the surfactant Tween80 and, as an example, the DTG curves of the blends 50:50 and 80:20 with and without surfactant.

INSERT FIGURE 4 ABOUT HERE

From this figure, it can be observed that the hybrid fibers presented a degradation profile intermediate between that of pure API and pullulan and, of course, dependent on the specific blend composition. In general, as observed in Table 2, the thermal stability of the

hybrid fibers was better than that of the pure protein, and the peak onset increased with surfactant addition, which in accordance to FTIR data, seems to indicate improved interactions between the protein and carbohydrate fractions, leading to enhanced thermal stability. In the electrospun fibers containing Tween80, a second degradation peak was apparent, which corresponded to the degradation of the surfactant.

INSERT TABLE 2 ABOUT HERE

**3.6 Effect of Relative Humidity (RH) and water resistance of the electrospun fibers**

The effect of relative humidity on the integrity of the electrospun fibers is important from a practical application viewpoint and, also, will influence the controlled release of potential encapsulated substances. Both the effect of relative humidity and water resistance was evaluated on two different fiber compositions, i.e. 50:50 and 80:20 with Tween80. Not surprisingly, it was seen that the fibers with greater carbohydrate content (API:pullulan 50:50) were less stable when exposed at 100% RH.. The fibers with greater pullulan content were somehow collapsed and thicker (probably due to swelling) while those with greater protein content maintained their integrity (see Figure A.3 in the Appendices). Table 3 compiles the weight loss of the 2 fiber compositions after water immersion during 5, 20, 30 and 60 minutes.

INSERT TABLE 3 ABOUT HERE

The carbohydrate polymer pullulan, and the surfactant Tween80 were the compounds of the fiber blends with greater water solubility. Therefore, considering 1 mg of electrospun

fibers, the theoretical pullulan+Tween80 content for the 50:50T and 80:20T compositions were of 0.55 mg and 0.31 mg, respectively. This amount is similar to the weight loss of the fibers after 60 minutes, which seems to indicate that the most hydrophilic fractions were lost upon water immersion. In fact, a considerable decrease in the characteristic bands from both pullulan and Tween80 was observed through FTIR spectroscopy as it can be observed in Figure 5 (cf. arrows).

INSERT FIGURE 5 ABOUT HERE

The ratio between the intensity of bands from the amide II (belonging to the API protein) and the band from the α-glucopyranoside units from pullulan (at ~850 $cm^{-1}$) was 4.27 and 4.18 for the 50:50T and 80:20T blends, respectively, i.e. more or less coincident with the ratio from the pure API (cf. Figure A.2 in the Appendices), thus confirming that the other two compounds were fully solubilized in water. These results, as commented before, may be interesting for controlled release applications of these structures, as it is anticipated that hydrophilic encapsulated compounds will be faster released from the 50:50T structures through the spaces left by the carbohydrate and surfactant compounds.

## 4. Conclusions

Ultrathin electrospun fibers from API-pullulan composite dispersions in formic acid have been developed for the first time using electrospinning. The study illustrated that electrospun fibers from edible biopolymers could be fabricated through addition of surfactant to modulate the solution properties. This study has also demonstrated that the

ability to generate encapsulation structures from API depends, not only on the protein conformation, but also on the solution properties (conductivity, surface tension and viscosity). The addition of pullulan was key for fiber development, but in the case of the blends with greater protein contents, a certain amount of surfactant was required to obtain defect-free fibers, fact that was related to α-helical conformation of the protein chains, as deduced from FTIR. The thermal stability was slightly increased in the hybrid fibers in comparison with the pure API structures, while the sensibility to water was highly dependent on the fiber composition.

**Acknowledgements**

The authors acknowledge Dr. Benito Manrique de Lara y Soria for providing the amaranth protein concentrate used in this study. A. Lopez-Rubio is recipient of a Ramon y Cajal contract from the Spanish Ministry of Science and Innovation. The authors thank the Spanish MINECO projects AGL2012-30647, FUN-C-FOOD (CSD2007-00063), and Mexican project FOMIX-QRO-2011-C02-175350 for financial support and Mexican National Council for Science and Technology (CONACYT) for a graduate fellowship, to author Marysol Aceituno-Medina.

## References


Aceituno-Medina, M., Lopez-Rubio, A., Mendoza, S., Lagaron, J.M. (2013). Development of novel ultrathin structures based in amaranth (*Amaranthus hypochondriacus*) protein isolate through electrospinning. *Food Hydrocolloids, 31*, 289-298.

Association of Official Analytical Chemists (1996). Official methods of analysis. 16th ed. AOAC, Arlington, VA.

Barth, A. (2007). Infrared spectroscopy of proteins. *Biochimica et Biophysica Acta (BBA) - Bioenergetics*, 1767, 1073-1101.

Bell, L.N. (2001). Stability testing of nutraceuticals and functional foods. In R.E.C. Wildman (Ed.), *Handbook of nutraceuticals and functional foods* (pp. 501-516). New York: CRC Press.

Buchko, C. J., Chen, L. C., Shen, Y., & Martin, D. C. (1999). Processing and microstructural characterization of porous biocompatible protein polymer thin films. *Polymer, 40*, 7397–7407.

Drzewiecki, J., Delgado-Licon, E., Haruenkit, R., Pawelzik, E., Martin-Belloso, O., Park, Y.-S., Jung, S.-T., Trakhtenberg, S., & Gorinstein, S. (2003). Identification and differences of total proteins and their soluble fractions in some pseudocereals based on electrophoretic patterns. *Journal of Agricultural and Food Chemistry, 51*, 7798-7804.

Gorinstein, S., Pawelzik, E., Delgado-Licon, E., Haruenkit, R., Weisz, M., & Trakhtenberg, S. (2002). Characterisation of pseudocereal and cereal proteins by protein and amino acid analyses. *Journal of the Science of Food and Agriculture, 82*, 886-891.

Gounga, M.E., Xu, S-Y., & Wang, Y. (2007).Whey protein isolate-based edible films as affected by protein concentration, glycerol ratio and pullulan addition in film formation. *Journal of Food Engineering, 73*(4), 155-161.

Heunis, T. D. J., Botes, M., & Dicks, L. M. T. (2010). Encapsulation of *Lactobacillus plantarum* 423 and its bacteriocin in nanofibers. *Probiotics and Antimicrobial Proteins, 2*, 46-51.

Jung, Y.H., Kim, H.Y., Lee, D.R., Park, S.Y. (2005). Characterization of PVOH nonwoven mats prepared from surfactant–polymer system via electrospinning. *Macromolecular Research, 13 (5)*, 385–390.

Karim, M.R., Lee, H.W., Kim, R., Ji, B.C., Cho,J.W., Son,T.W. Oh, W., Yeum, J.H. (2009). Preparation and characterization of electrospun pullulan/montmorillonite nanofiber mats in aqueous solution. *Carbohydrates polymers, 78*, 336-342.

Kimoto, T., Shibuya, T., Shiobara,S. (1997). Safety studies of a novel starch, pullulan: chronic toxicity in rats and bacterial mutagenicity. *Food Chemistry and Toxicology, 35*, 323-329.

Kriegel, C., Kit, K. M., McClements, D. J., & Weiss, J. (2009). Electrospinning of chitosan–poly(ethylene oxide) blend nanofibers in the presence of micellar surfactant solutions. *Polymer, 50*, 189–200.

Li, Y., Lim, L. T., & Kakuda, Y. (2009). Electrospun zein fibers as carriers to stabilize (−)-Epigallocatechin Gallate. *Journal of Food Science, 74*, 233-240.

Lopez-Rubio, A., Flanagan, B. M., Shrestha, A. K., Gidley, M. J., & Gilbert, E. P. (2008). Molecular rearrangement of starch during in vitro digestion: toward a better understanding of enzyme resistant starch formation in processed starches. *Biomacromolecules, 9*, 1951-1958.

Lopez-Rubio, A. & Lagaron, J. M. (2012). Whey protein capsules obtained through electrospraying for the encapsulation of bioactives. *Innovative Food Science and Emerging Technologies, 13*, 200-206.

Lopez-Rubio, A., Sanchez, E., Sanz, Y., & Lagaron, J. M. (2009). Encapsulation of living bifidobacteria in ultrathin PVOH electrospun fibers. *Biomacromolecules, 10*, 2823-2829.

Lopez-Rubio, A., Sanchez, E., Wilkanowicz, S., Sanz, Y., & Lagaron, J. M. (2012). Electrospinning as a useful technique for the encapsulation of living Bifidobacteria in food hydrocolloids. *Food Hydrocolloids, 28*, 159-167.

Martínez, E. N., & Añon, M. C. (1996). Composition and structural characterization of amaranth protein isolates. An electrophoretic and calorimetric study. *Journal of Agricultural and Food Chemistry*, *44*, 2523-2530.

McClements D. J. (2006). Non-covalent interactions between proteins and polysaccharides. *Biotechnology Advances, 24,* 621-625.

Nie, H., He, A., Zheng, J., Xu, S., Li, J., & Han, C. (2008). Effects of Chain Conformation and Entanglement on the Electrospinning of Pure Alginate. *Biomacromolecules*, *9* (5), 1362–1365.

Peng, H., Zhou, S., Guo, T., Li, Y., Li, X., Wang, J., & Weng, J. (2008). *In vitro* degradation and release profiles for electrospun polymeric fibers containing paracetamol. *Colloids and Surfaces B: Biointerfaces*, *66 (2),* 206–212.

Prasad, P., Guru, G. S., Shivakumar, H.R., & Sheshappa Rai, K. (2012). Investigation on miscibility of sodium alginate/pullulan blends. *Journal of Polymers and the Environment, 20,* 887-893.

Reneker, D. H., & Chun, I. (1996). Nanometre diameter fibers of polymer, produced by electrospinning. *Nanotechnology, 7*, 216-223.

Schnetzler, K. A., & Breen, W. M. (1994). Food uses and amaranth product research: A comprehensive review. In O. Paredes-Lopez (Ed.), *Amaranth: Biology, chemistry and technology* (pp. 155-184). CRC Press: Boca Raton, FL.

Teutónico, R. A., & Knorr, D. (1985). Nondestructive method for oxalate determination of cultured Amaranthus tricolor cells. *Journal of Agricultural and Food Chemistry, 33*, 60-62.

Tolstoguzov, V.B. (1991). Functional properties of food proteins and role of protein-polyssaccharide interaction. *Food Hydrocolloids*, *4*, 429-468.

Torres-Giner, S., Martinez-Abad, A., Ocio, M. J., & Lagaron, J. M. (2010). Stabilization of a nutraceutical omega-3 fatty acid by encapsulation in ultrathin electrosprayed zein prolamine. *Journal of Food Science, 75*, N69-N79.

Wongsasulak, S., Kit, K. M., McClements, D. J. Yoovidhya, T., & Weiss, J. (2007). The effect of solution properties on the morphology of ultrafine electrospun egg albumen-PEO composite fibers. *Polymer, 48*, 448-457.

Wongsasulak, S., Patapeejumruswong, M., Weiss, J., Supaphol, P., & Yoovidhya, T. (2010). Electrospinning of food-grade nanofibers from cellulose acetate - egg albumen blends. *Journal of Food Engineering, 98*, 370-376.

Wu, J., Zhong, F., Li, Y., Shoemaker, C. F., & Xia, W. (2013). Preparation and characterization of pullulan-chitosan and pullulan-carboxymethyl chitosan blended films. *Food Hydrocolloids, 30*, 82-91.

Yoneyama M., Okada K., Mandai T., Aga H., Sakai S., & Ichikawa T. (1990). Effects of pullulan intake in humans. *Journal of the Japanese Society of Starch Science, 37*, 123-127.

## Appendices

a)

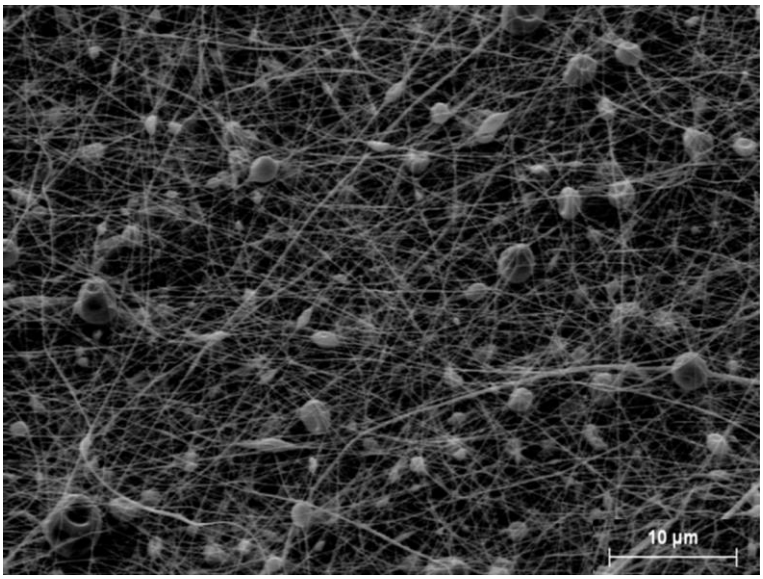


b)

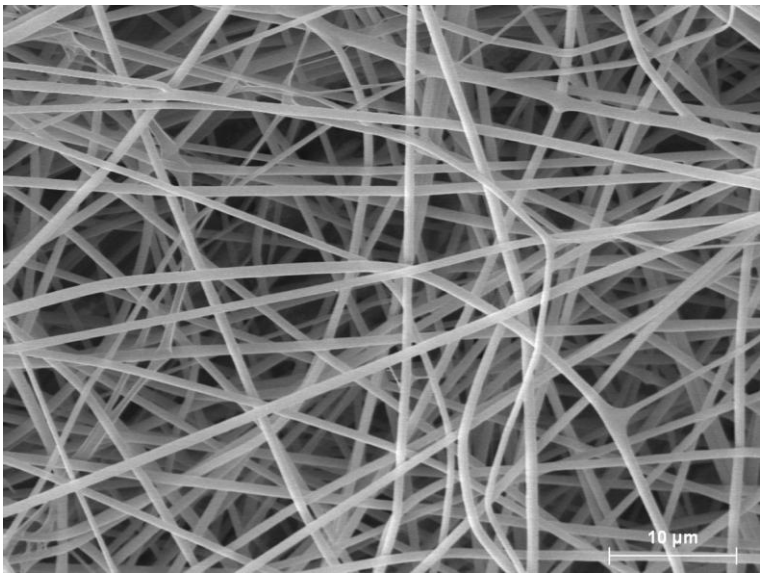


**Figure A.1.** SEM images of a) 10% (w/v) pullulan and b) 20% (w/v) pullulan, in 95% formic acid. Scale bar: 10 µm.

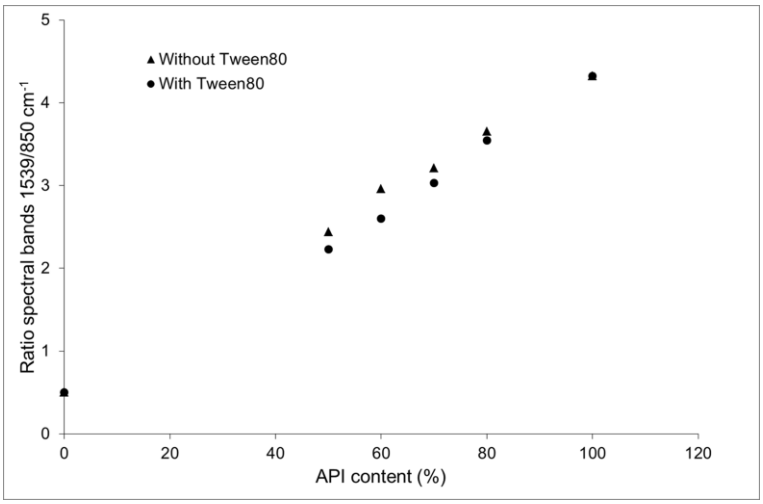


**Figure A.2.** Ratio of the spectral bands at 1539 $cm^{-1}$ (from API) and at 850 $cm^{-1}$ (from pullulan) for the various electrospun fibers with and without surfactant.

a)

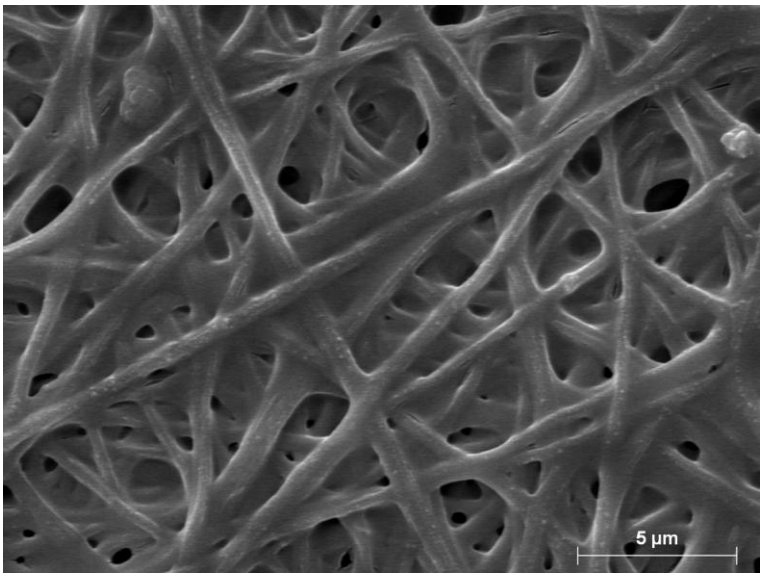


b)

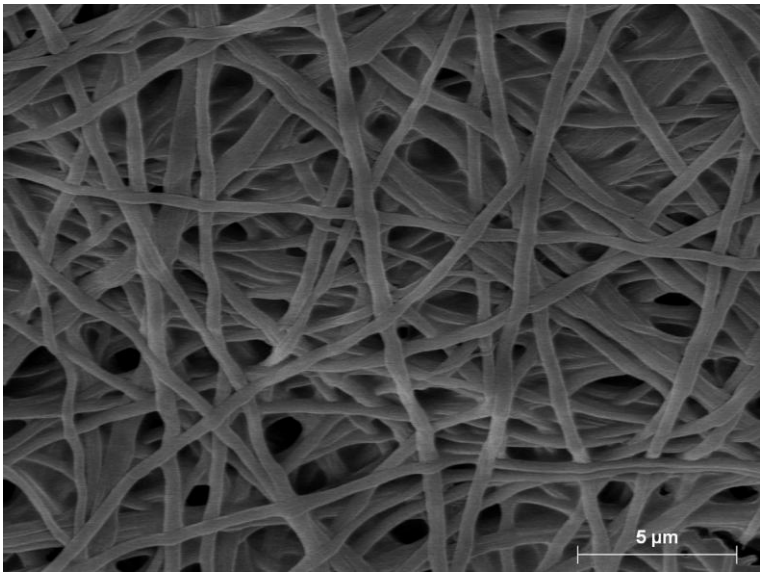


**Figure A.3.** SEM images of API:pullulan fibers with Tween 80 after 30 minutes of exposure to 100% RH: a) 50:50, b) 80:20. Scale bar: 5 µm.

**Figure captions.**

**Figure 1.** SEM images of electrospun API:pullulan blend structures at the following ratios: A) 50:50; B) 50:50 with Tween80; C) 60:40; D) 60:40 with Tween80; E) 70:30; F) 70:30 with Tween80; G) 80:20; H) 80:20 with Tween80. Scale bar: 5 µm.

**Figure 2.** Infrared absorbance spectra of different electrospun structures: A) API; B) Pullulan; C) API:pullulan 50:50; D) API:pullulan 50:50 with Tween80; E) API:pullulan 80:20; F) API:pullulan 80:20 with Tween80. Dashed line indicates the maximum of the NH stretching band for API and arrows point out the bands that were used to qualitatively estimate the composition of the fibers. Spectra have been offset for clarity.

**Figure 3.** FTIR spectra in the range of the amide I and II bands for pure API fibers (thicker solid line), and API:pullulan blends: 50:50, 50:50 with Tween80, 60:40, 60:40 with Tween80 (solid lines), 70:30 (grey line), 70:30 with Tween80 (dotted line), 80:20 (dashed line) and 80:20 with Tween80 (dash-dot-dot line). Spectra have been normalized to the amide I band for better comparison.

**Figure 4.** DTG curves of pure API, pullulan, Tween80 and of the hybrid API:pullulan fibers: 50:50, 50:50 with Tween80, 80:20 and 80:20 with Tween80.

**Figure 5.** Infrared absorbance spectra of API:pullulan blend structures: A) 50:50 with Tween80; B) 50:50 with Tween80 after 60 minutes in water; C) 80:20 with Tween80; D) 80:20 with Tween80 after 60 minutes in water. Arrows point out the decrease of characteristic bands from pullulan and Tween80. Spectra have been offset for clarity.

**Figure Captions (Appendices)**

**Figure A.1.** SEM images of a) 10% (w/v) pullulan and b) 20% (w/v) pullulan, in 95% formic acid. Scale bar: 10 µm.

**Figure A.2.** Ratio of the spectral bands at 1539 $cm^{-1}$ (from API) and at 850 $cm^{-1}$ (from pullulan) for the various electrospun fibers with and without surfactant.

**Figure A.3.** SEM images of API:pullulan fibers with Tween 80 after 30 minutes of exposure to 100% RH: a) 50:50, b) 80:20. Scale bar: 5 µm.

**Figure 1A**

**Click here to download high resolution image**

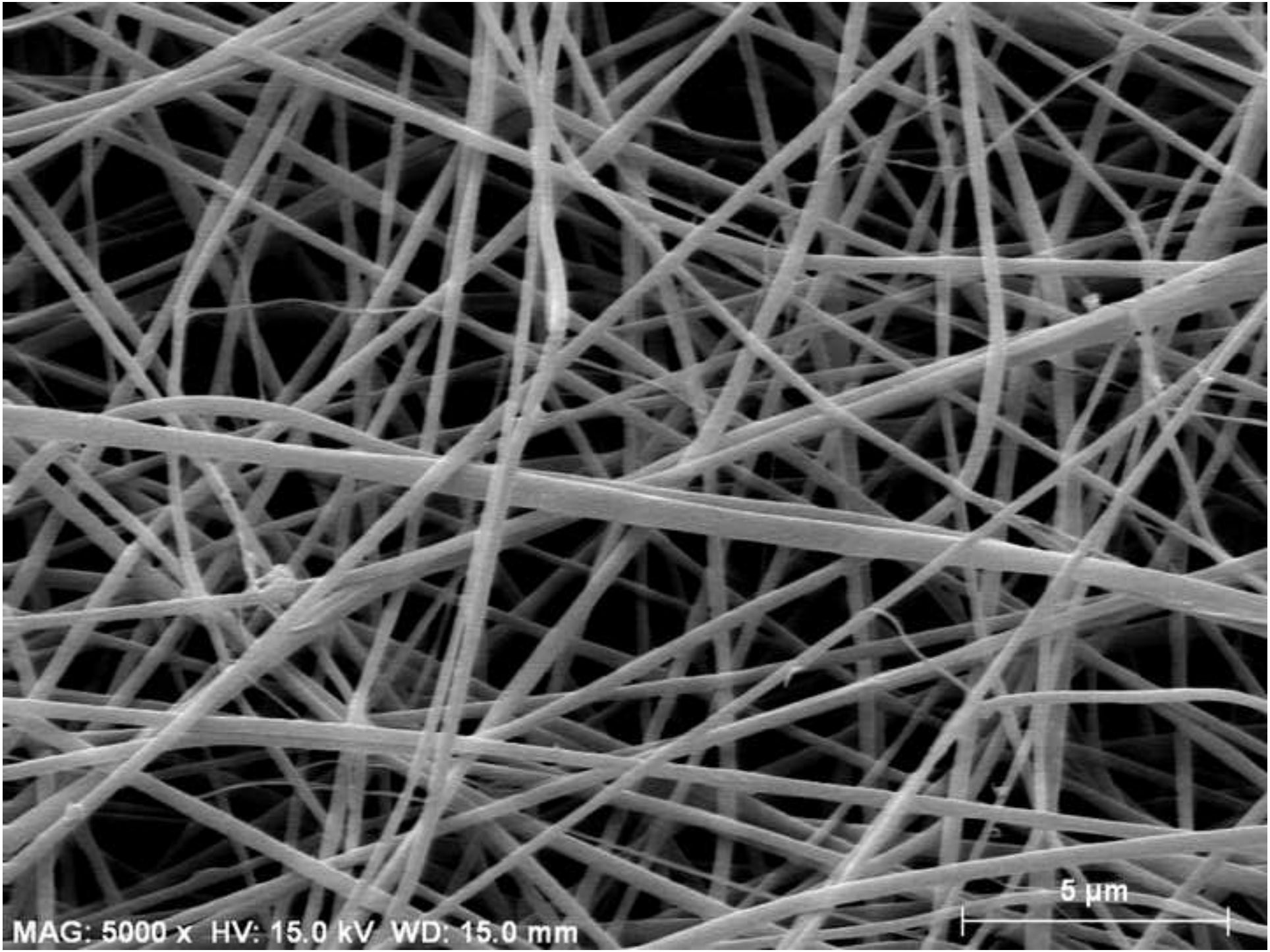

**Figure 1B**

Click here to download high resolution image

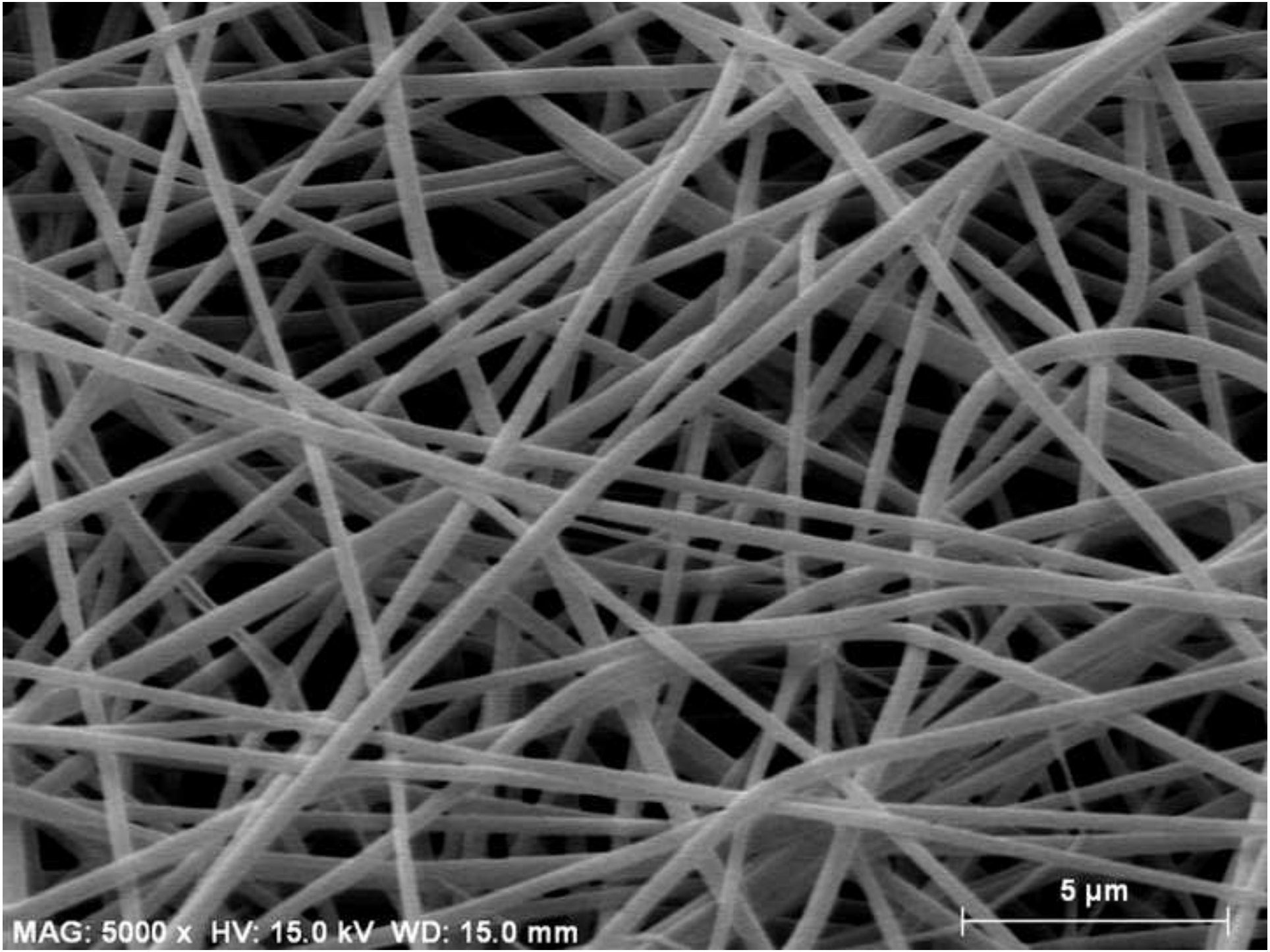

**Figure 1C**

**Click here to download high resolution image**

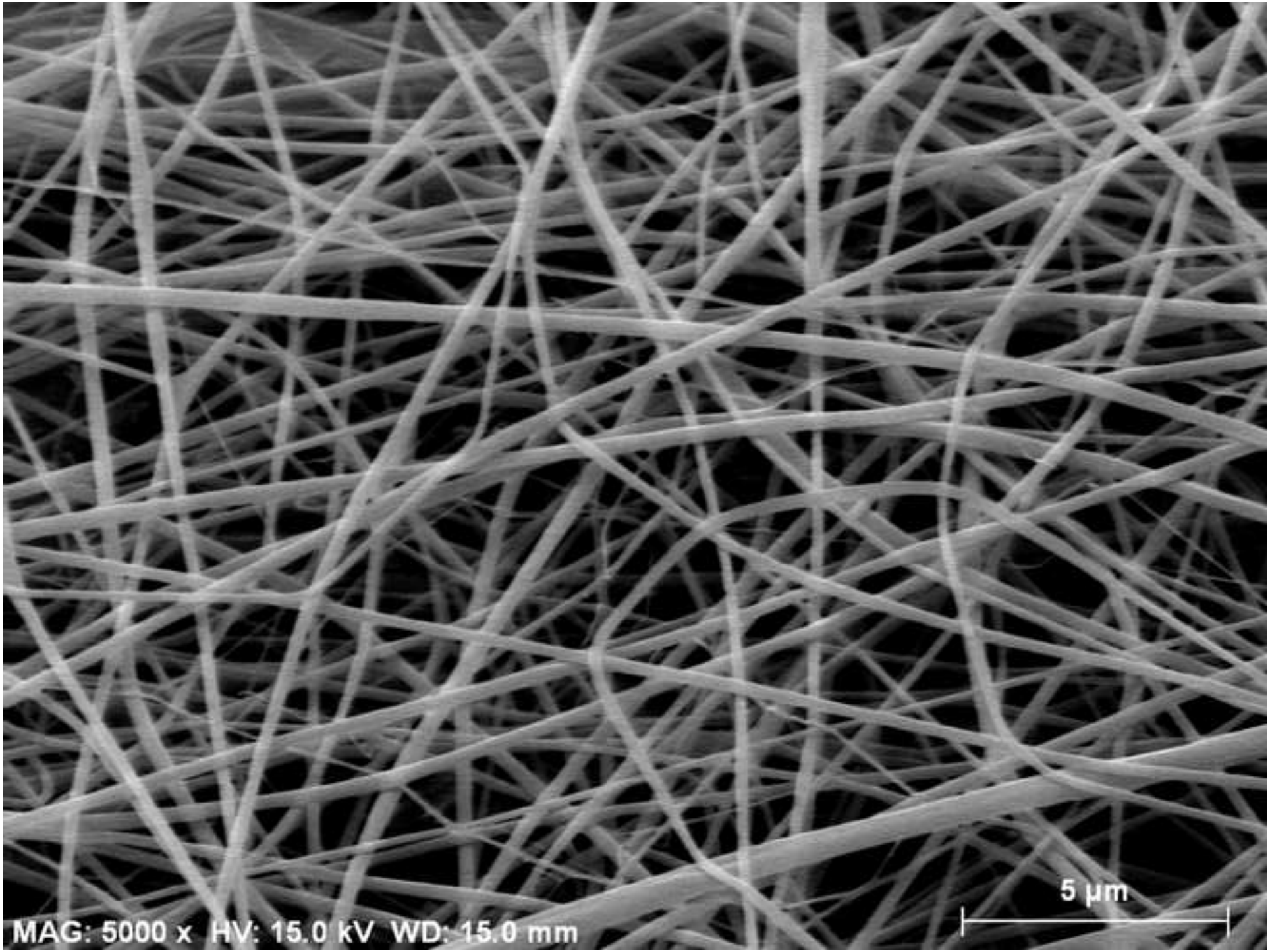

**Figure 1D**

**Click here to download high resolution image**

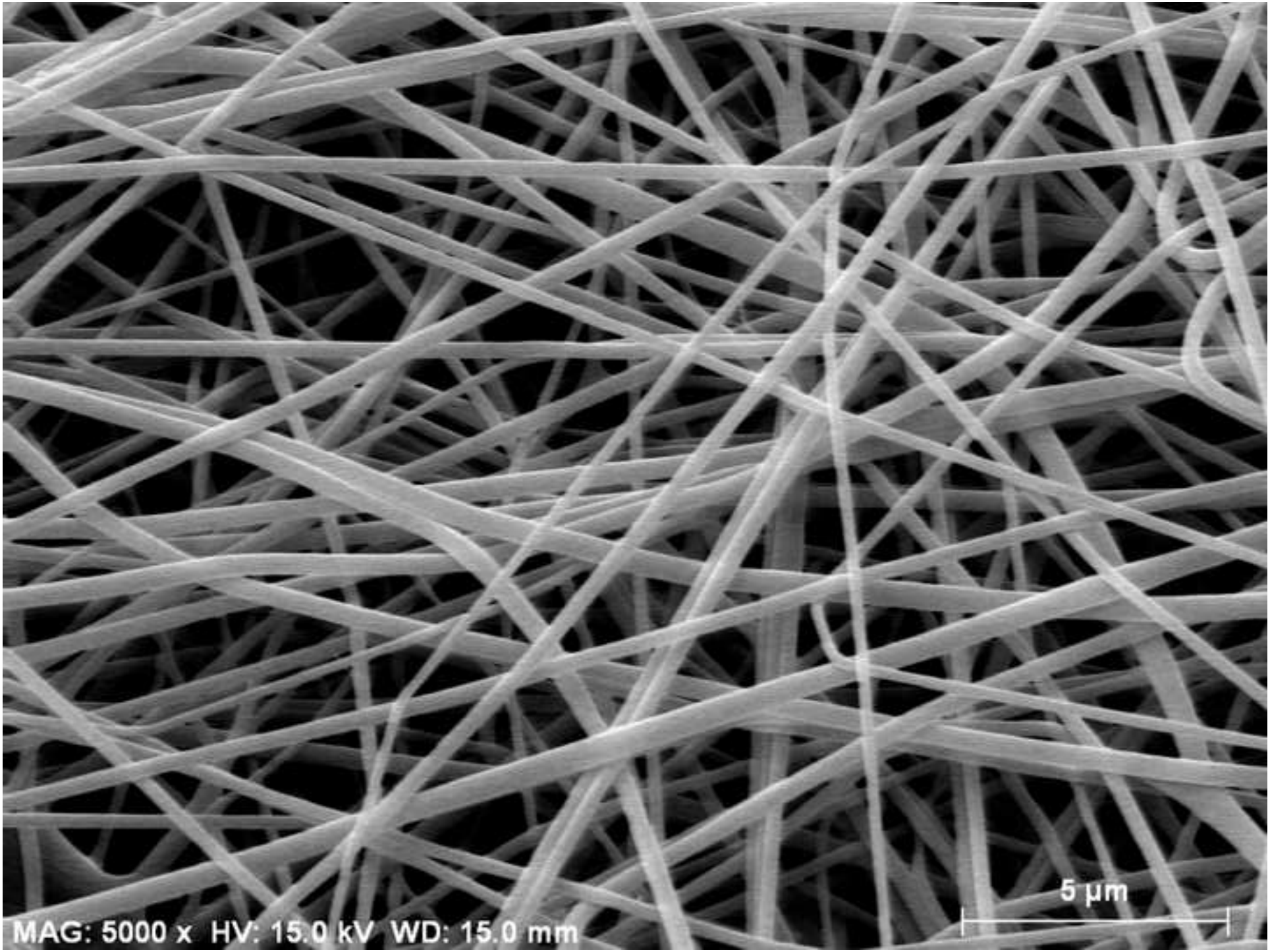

**Figure 1E**

**Click here to download high resolution image**

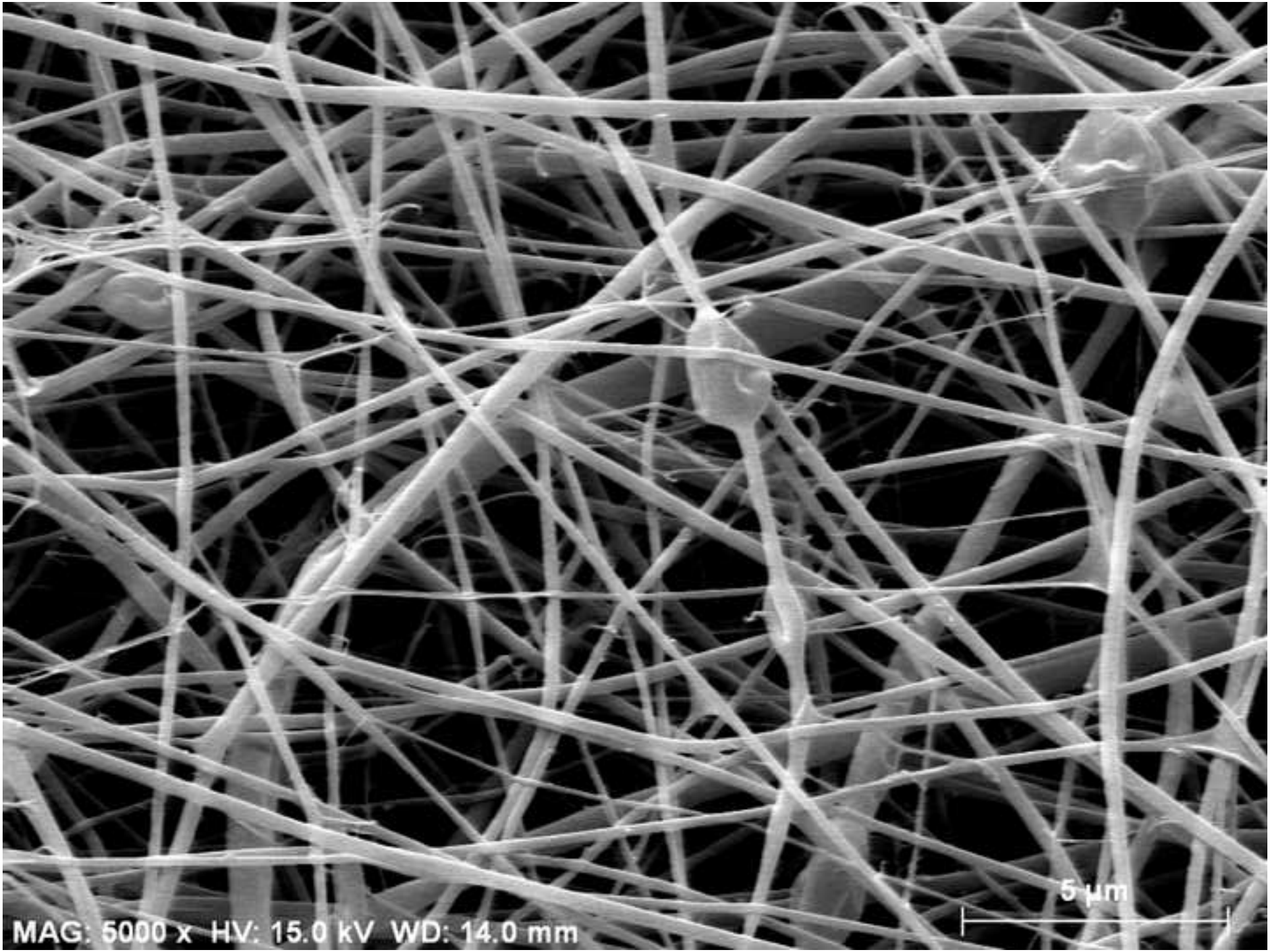

**Figure 1F**

Click here to download high resolution image

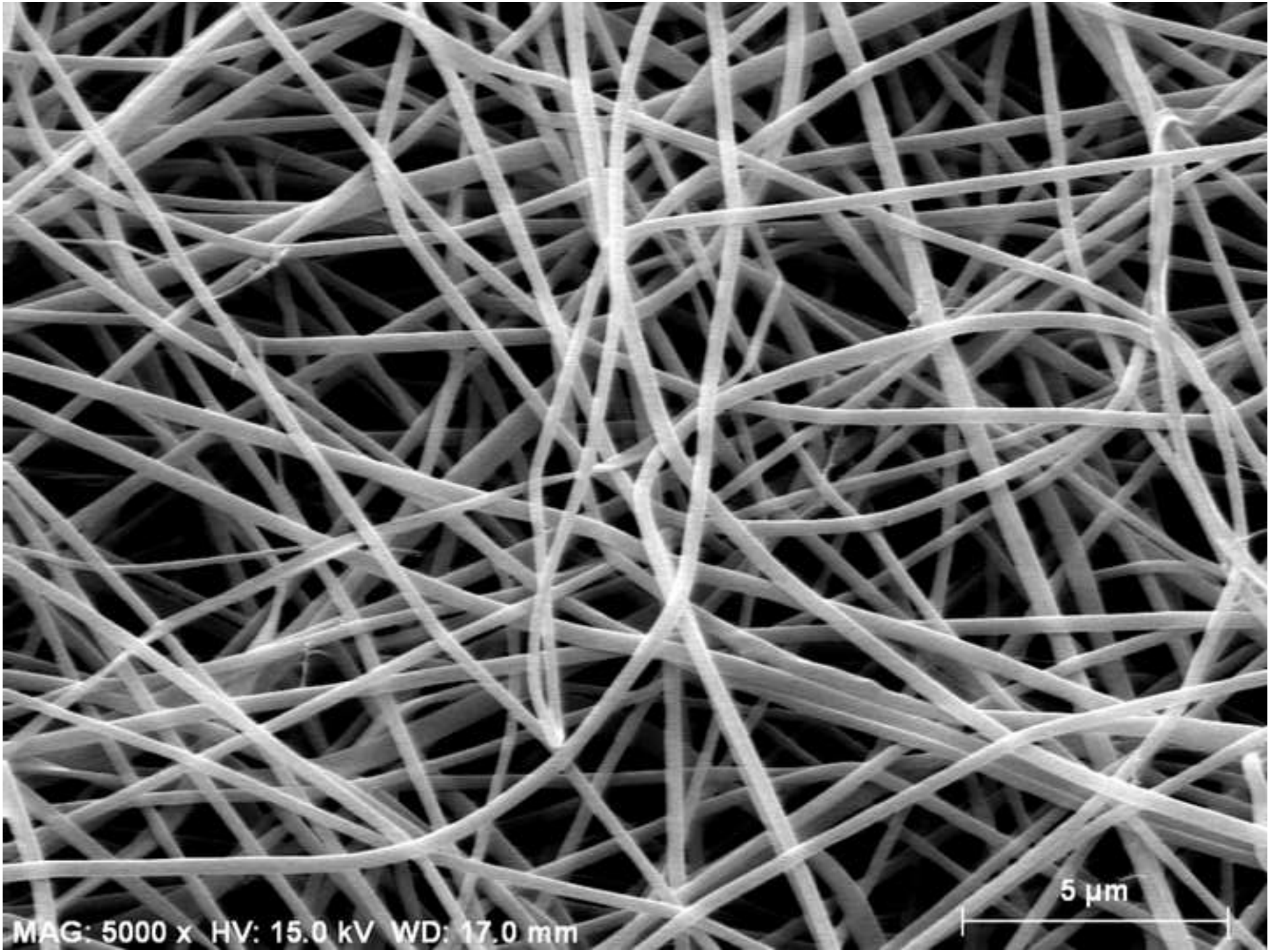

**Figure 1G**

**Click here to download high resolution image**

**Figure 1H**

**Click here to download high resolution image**

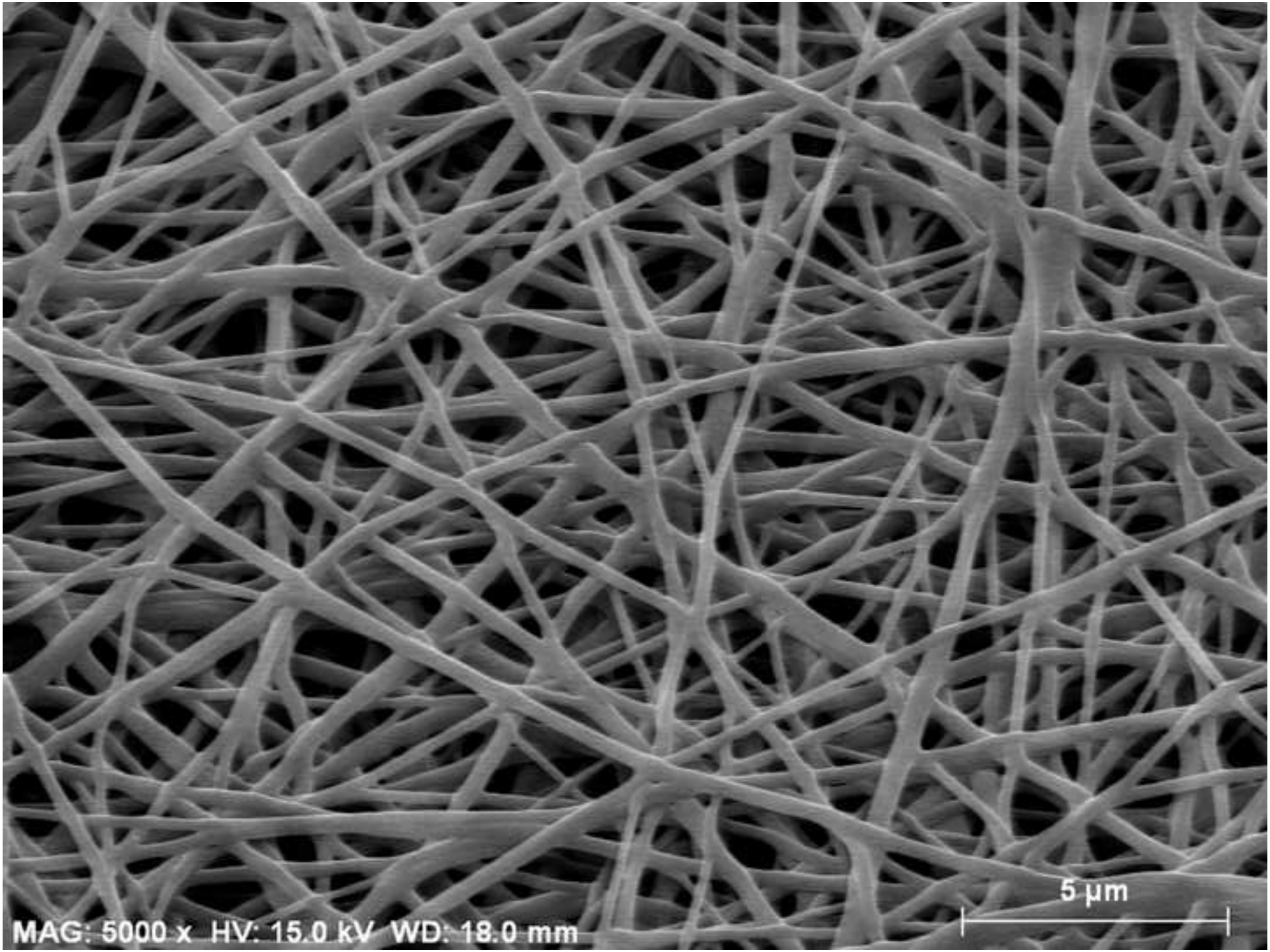

**Figure 2**

**Click here to download high resolution image**

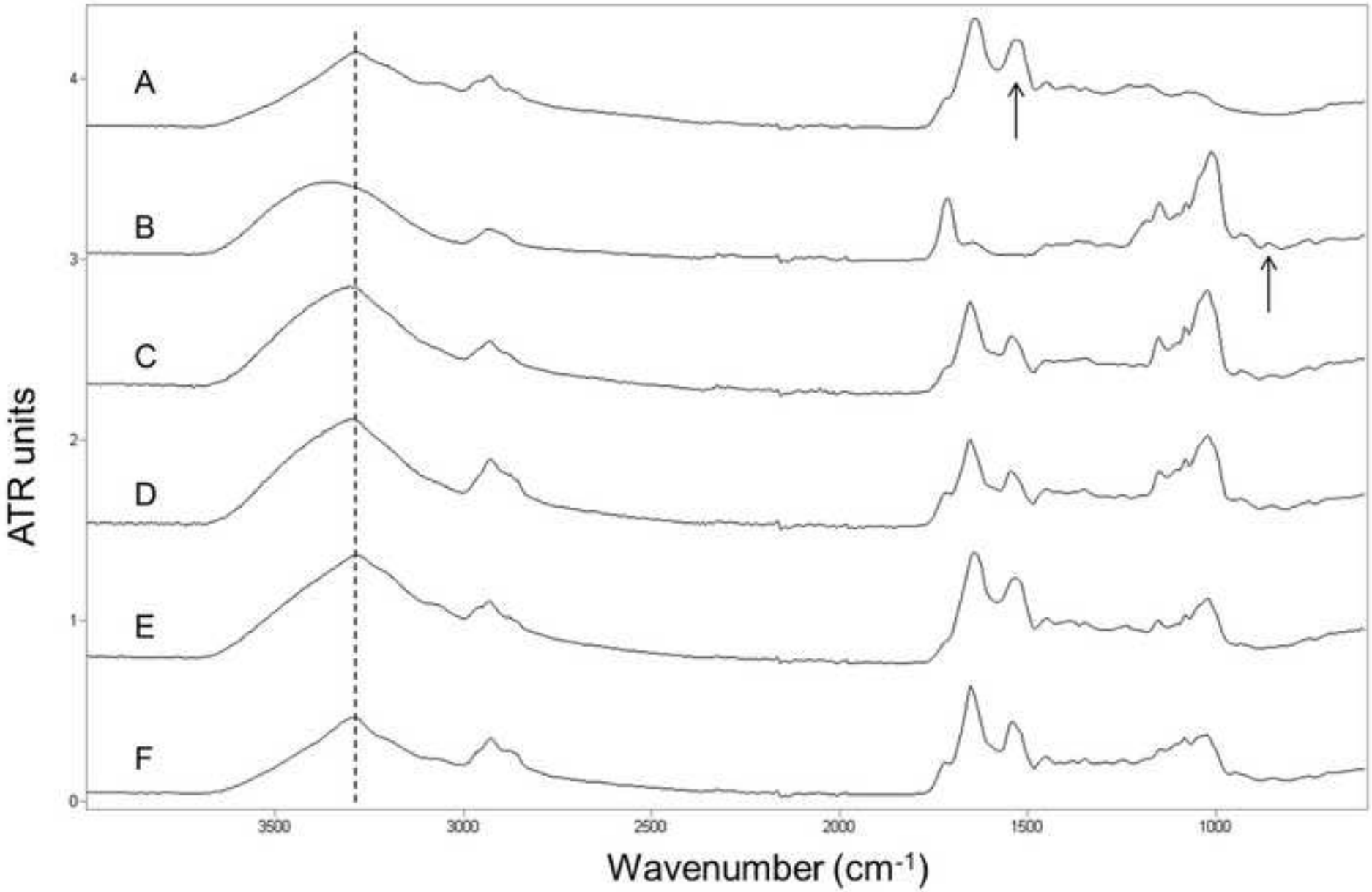

**Figure 3**

Click here to download high resolution image

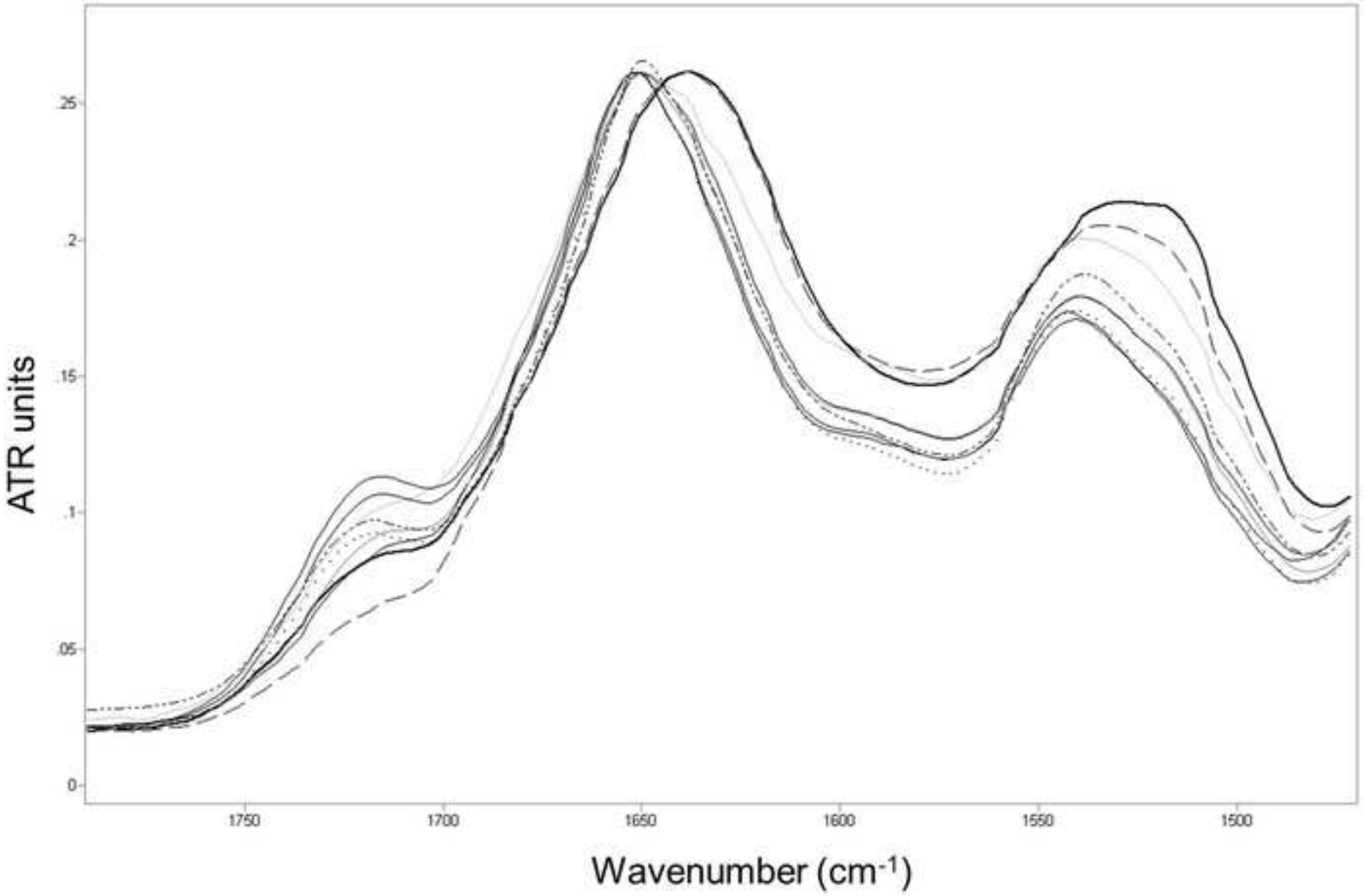

**Figure 4**

**Click here to download high resolution image**

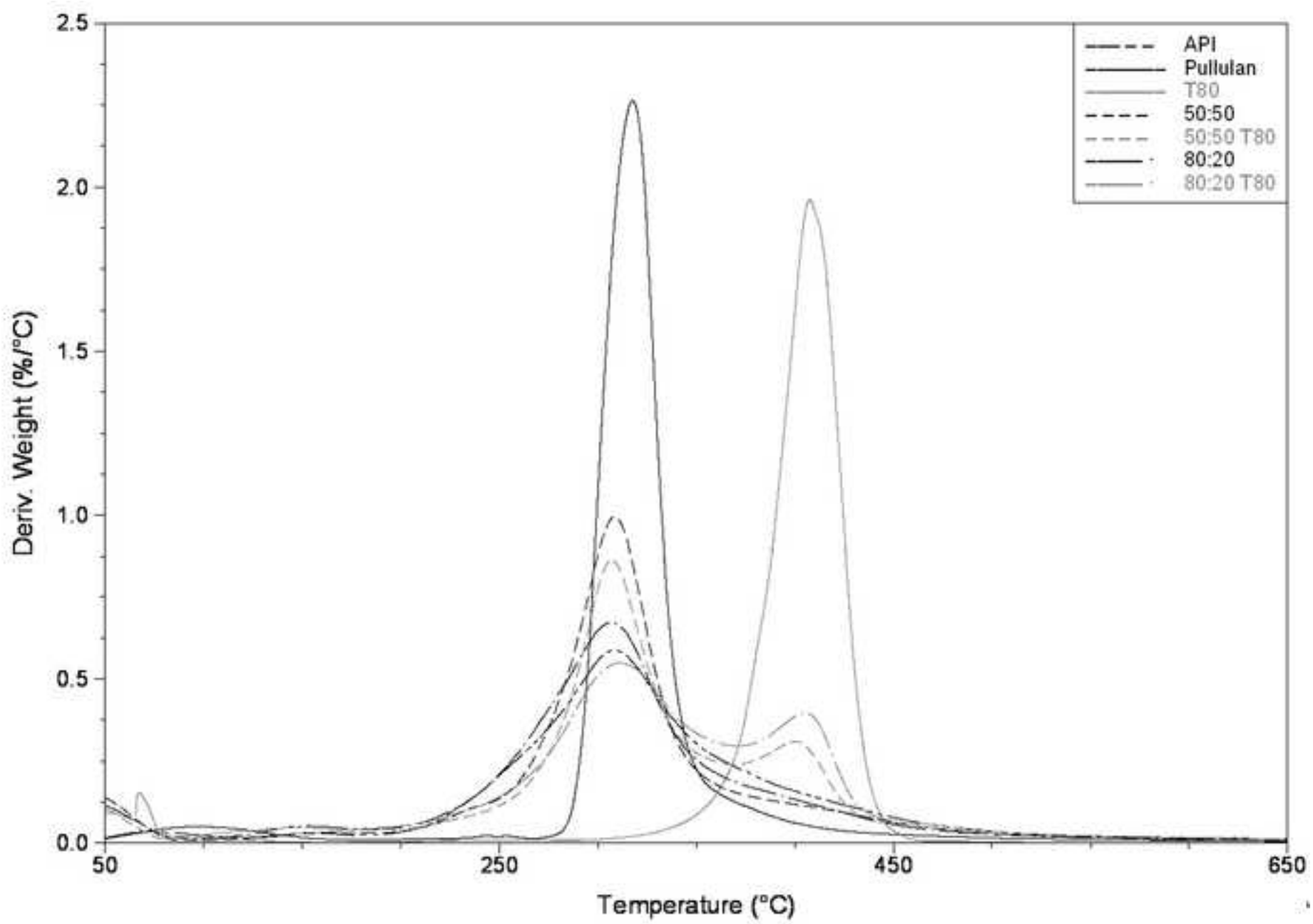

**Figure 5**

Click here to download high resolution image

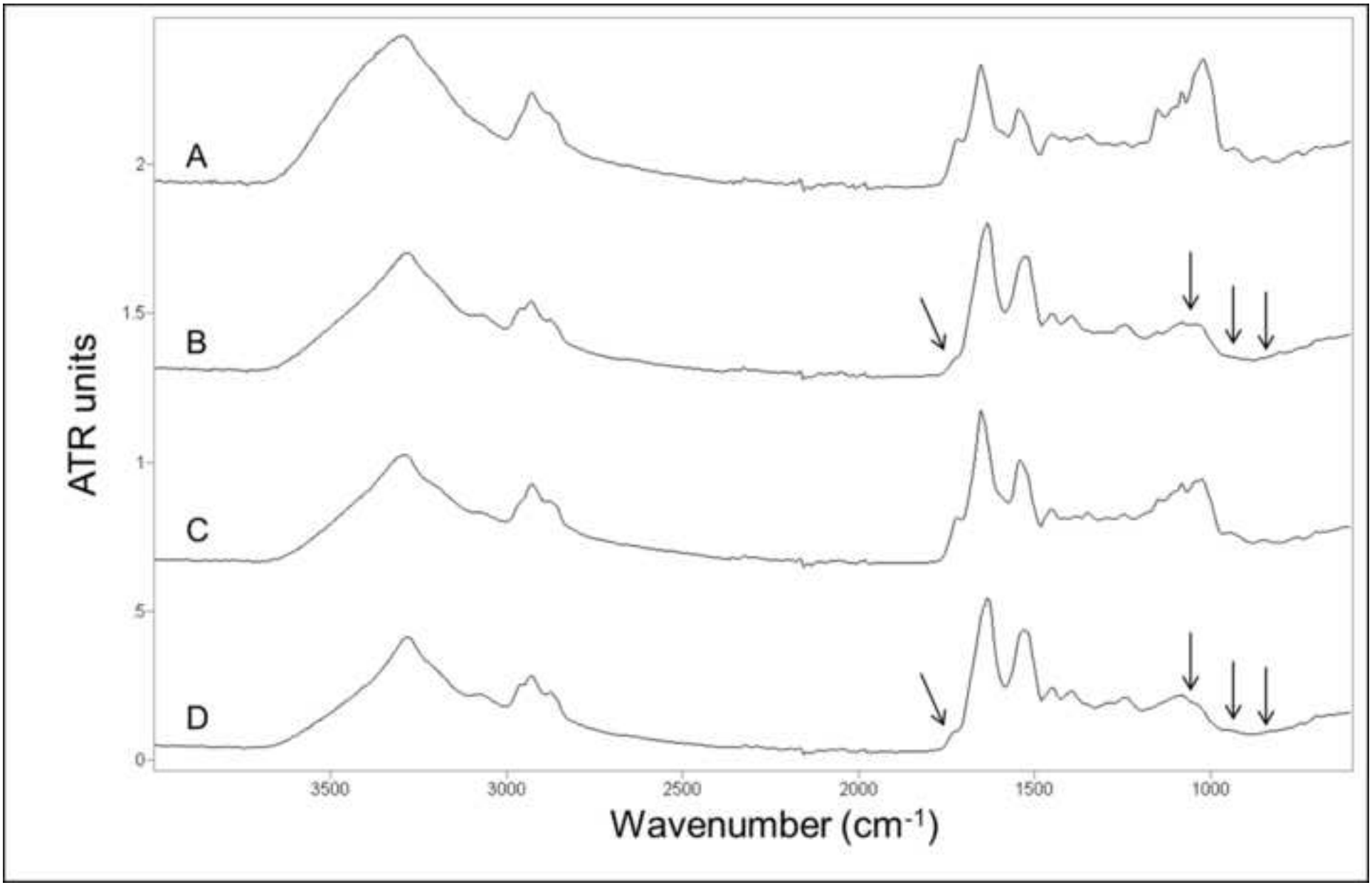

**Table 1.** Apparent viscosity, conductivity and surface tension of the various API:pullulan solutions and diameter of the electrospun fibers obtained thereof.

| API: Pullulan | Apparent viscosity (cP) | Conductivity (mS/cm) | Surface tension (mN/m) | Morphology | Diameter (nm) |
|---|---|---|---|---|---|
| 50:50 | $560,5 \pm 15,2^{a}$ | $5,8 \pm 0,3^{ab}$ | $32,1 \pm 0,4^{a}$ | Fibers | $266,6 \pm 80,1^{a}$ |
| 50:50T | $587,6 \pm 18,1^{a}$ | $5,4 \pm 0,2^{a}$ | $31,0 \pm 0,9^{a}$ | Fibers | $352,5 \pm 60,7^{a}$ |
| 60:40 | $478,4 \pm 10,3^{b}$ | $6,1 \pm 0,1^{abc}$ | $30,9 \pm 0,1^{a}$ | Fibers | $226,9 \pm 140,2^{ab}$ |
| 60:40T | $496,6 \pm 3,3^{b}$ | $5,9 \pm 0,3^{ab}$ | $32,0 \pm 0,3^{a}$ | Fibers | $339,9 \pm 82,2^{a}$ |
| 70:30 | $356,8 \pm 5,9^{c}$ | $6,5 \pm 0,4^{bc}$ | $31,5 \pm 0,6^{a}$ | Beaded fibers | $261,6 \pm 292,5^{b}$ |
| 70:30T | $366,1 \pm 6,6^{c}$ | $6,3 \pm 0,3^{bc}$ | $32,1 \pm 0,3^{a}$ | Fibers | $299,9 \pm 60,5^{a}$ |
| 80:20 | $312,7 \pm 2,2^{d}$ | $6,8 \pm 0,2^{c}$ | $32,4 \pm 0,8^{a}$ | Beaded fibers | $1708,3 \pm 1831,2^{c}$ |
| 80:20T | $362,5 \pm 3,9^{c}$ | $6,7 \pm 0,1^{c}$ | $31,9 \pm 0,7^{a}$ | Fibers | $305,1 \pm 71,1^{a}$ |

a-d different superscripts within the same column indicate significant differences among samples ($p<0.05$).

"T" refers to the solutions containing Tween80

**Table 2**. TGA maximum of the weight loss first derivate ($T_D$) and the corresponding peak onset values and the residue at 600 °C for pure API, pullulan, Tween80 and the hybrid electrospun structures

| Samples | Onset T (ºC) | $T_D$ (ºC) | Residue at 600ºC (%) |
|---|---|---|---|
| API | 242,9 | 308,5 | 23,6 |
| Pullulan | 290,6 | 317,5 | 8,3 |
| Tween80 | 376,2 | 407,4 | 17,6 |
| API:Pullulan 50:50 | 267,9 | 308,3 | 17,1 |
| API:Pullulan 50:50T | 273,3 | 306,9 | 17,3 |
| | | 401,1 | |
| API:Pullulan 60:40 | 264,2 | 307,9 | 17,6 |
| API:Pullulan 60:40T | 269,6 | 303,1 | 17,9 |
| | | 400,3 | |
| API:Pullulan 70:30 | 254,7 | 307,6 | 17,3 |
| API:Pullulan 70:30T | 263,7 | 306,7 | 15,5 |
| | | 402,8 | |
| API:Pullulan 80:20 | 243,5 | 306,7 | 21,1 |
| API:Pullulan 80:20T | 263,5 | 310,9 | 19,1 |
| | | 407,3 | |

**Table 3.** Fiber weight loss after immersion in water for 5, 20, 30 and 60 min.

| API: Pullulan | Immersion time (minutes) | Initial weight (mg) | Final weight (mg) | Weight loss (mg) |
|---|---|---|---|---|
| 50:50T | 5 | 1,0 | 0,93 ± 0,01 | 0,07 ± 0,01 |
| | 20 | 1,0 | 0,84 ± 0,01 | 0,16 ± 0,01 |
| | 30 | 1,0 | 0,60 ± 0,02 | 0,40 ± 0,02 |
| | 60 | 1,0 | 0,47 ± 0,01 | 0,53 ± 0,01 |
| 80:20T | 5 | 1,0 | 0,97 ± 0,01 | 0,03 ± 0,01 |
| | 20 | 1,0 | 0,89 ± 0,02 | 0,11 ± 0,02 |
| | 30 | 1,0 | 0,79 ± 0,01 | 0,19 ± 0,01 |
| | 60 | 1,0 | 0,72 ± 0,02 | 0,28 ± 0,02 |

"T" refers to the structures containing Tween80

**Figure A.1a**

**Click here to download Supplementary Data: FIGURE A.1a.tif**

**Figure A.1b**

**Click here to download Supplementary Data: FIGURE A.1b.tif**

**Figure A.2**

**Click here to download Supplementary Data: FIGURE A.2.tif**

**Figure A.3a**

**Click here to download Supplementary Data: FIGURE A.3a.tif**

**Figure A.3b**

**Click here to download Supplementary Data: FIGURE A.3b.tif**